Mixing of passive tracers at the ocean surface and its implications for plastic transport modelling

Environmental Research Communications

PAPER

Mixing of passive tracers at the ocean surface and its implications for plastic transport modelling

David Wichmann[1,2], Philippe Delandmeter[1], Henk A Dijkstra[1,2] and Erik van Sebille[1,2]

[1] Institute for Marine and Atmospheric research Utrecht, Utrecht University, Princetonplein 5, 3584 CC Utrecht, The Netherlands
[2] Centre for Complex Systems Studies, Utrecht University, Leuvenlaan 4, 3584 CC Utrecht, The Netherlands

E-mail: d.wichmann@uu.nl

Keywords: microplastic, Lagrangian particle tracking, Markov chains, mixing time, mixing entropy

Supplementary material for this article is available online

OPEN ACCESS

RECEIVED
7 June 2019

REVISED
13 October 2019

ACCEPTED FOR PUBLICATION
16 October 2019

PUBLISHED
29 October 2019

Abstract

The tracking of virtual particles is one of the main numerical tools to understand the global dispersion of marine plastic debris and has been successful in explaining the global-scale accumulation patterns of surface microplastic, often called 'garbage patches'. Yet, the inherent inaccuracies in plastic input scenarios and ocean circulation model results produce uncertainties in particle trajectories, which amplify due to the chaotic property of the surface ocean flow. Within this chaotic system, the subtropical 'garbage patches' correspond to the attractor. These facts make the large scale surface ocean circulation a mixing dynamical system, which means that the information of a particle's initial location is lost over time. We use mixing entropy and Markov chain mixing of the transfer operator associated with surface ocean transport to quantify the time scales of mixing for the global surface ocean in each subtropical basin. In the largest parts of all basins we find mixing times in the order of or below 10 years, which is lower than typical simulation times for surface plastic transport simulations. Maximum mixing times of more than 10 years are found in some parts of the North and South Pacific. Our results have important implications for global dispersion modelling of floating materials on the basin scale: precise initial information has little relevance for long term simulations, and there is a temporal limit after which the backtracking of particles is not meaningful any more.

1. Introduction

Plastic debris is very common in today's marine environment. It can be found in the open ocean and on beaches, but also in more remote habitats such as the polar regions and deep sea sediments [1–4]. Sources of debris can be land based (e.g. river mouths) or marine (e.g. shipping vessels) [3, 5, 6]. Once in the ocean, buoyant plastic debris can be transported over large distances by the surface ocean currents. An important tool to understand these pathways on the global scale has been numerical modelling [7], mostly Lagrangian particle tracking. Most of the currently existing numerical studies restrict themselves to the surface ocean, and they successfully reproduce the large scale features of surface microplastic distributions, which are the accumulation patterns in each individual subtropical gyre [8–13]. Figure 1 shows the result of a typical simulation of an initially uniform particle distribution after 10 years (see section 2 for simulation details). The high concentrations in the subtropical gyres are mainly caused by the converging Ekman currents in the subtropics [14, 15] and are often called 'garbage patches'.

The success of these surface transport simulations is to some extent surprising. Recent experimental and theoretical studies clearly suggest that initially buoyant microplastic particles are likely to sink due to biofouling [16–18], such that the actual particle dynamics is unlikely to be well-represented by surface transport alone. Furthermore, the accumulation in the subtropical gyres is a feature that is present in long term distributions of different modeling studies that use different initial particle input scenarios (e.g. uniform, realistic, release at once or continuous) and different circulation models [8–12]. The presence of large scale robust features in different

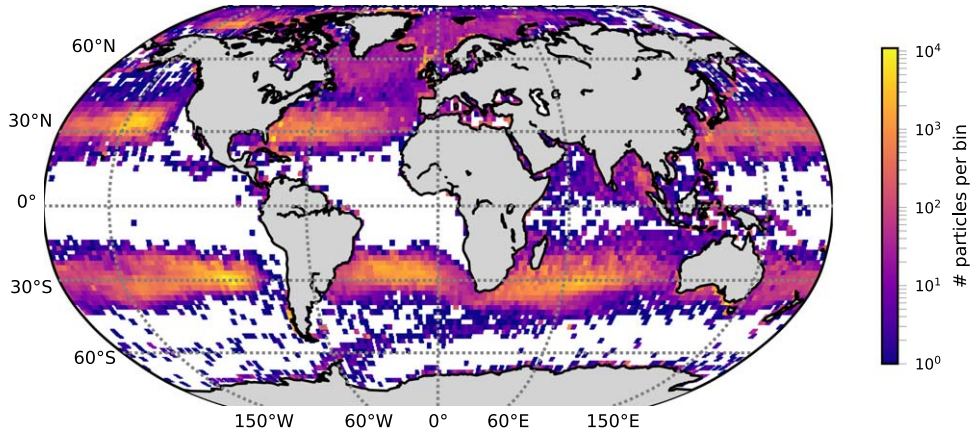

Figure 1. Concentration of approximately 1 million initially uniformly distributed particles after 10 years. The concentration (logarithmic scale) is computed with a 2° square binning. The converging Ekman currents in the subtropics lead to the accumulation of particles in these regions, called garbage patches. The simulation details are described in section 2.

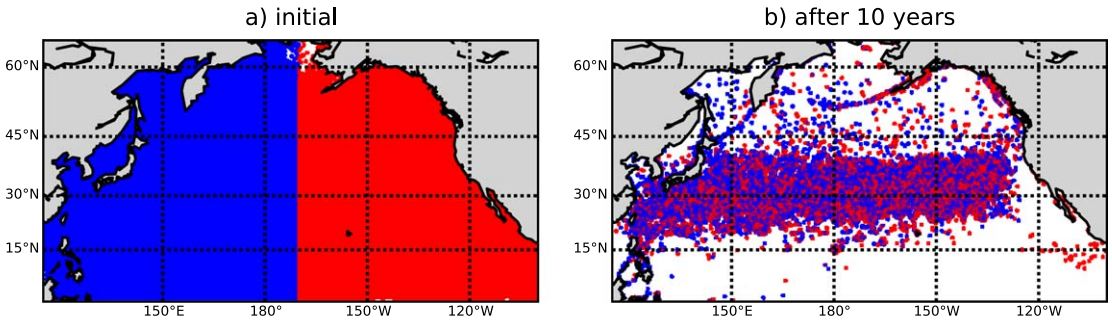

Figure 2. Initial and final positions of particles that are coloured according to their initial position. The red and blue particles are apparently completely mixed after 10 years in the centre of the subtropical gyre. We refer for simulation details to section 2.

models to some extend seems to argue against the usage of realistic, small-scale input scenarios to model long term global plastic distributions, e.g. based on population densities [8, 10]. Particles seem to accumulate in similar regions in the long run, with the particle history only playing a minor role.

In this article, we address this issue: our hypothesis is that the surface ocean current in each basin is *mixing* on time scales of several years, which is in the order of typical time scales of interest for global plastic transport modelling. The mixing property means that individual surface particles 'forget' their history, and *particle densities*, i.e. particle distributions normalised to unity, converge to the subtropical accumulation regions almost independently of initial conditions or small perturbations of the flow, such as sub-surface advection. The basic idea is illustrated in figure 2, that shows the initial (a) and final (b) positions of virtual particles as a scatter plot in the North Pacific. In the figure, particles originating from the eastern and western parts of the basin are labelled with different colours. While there are a few regions (mostly close to coasts) that remain dominantly red or blue, the colours apparently have completely mixed within the centre of the basin after 10 years.

For the application we present here, the property of 'history loss' of an individual particle results from the combination of two features that are inherent to all simulations using Lagrangian particle tracking on the oceanic scale: the chaotic behaviour of trajectories, and the finite accuracy of ocean circulation models. For plastic modelling, plastic input scenarios are an additional source of uncertainty. The chaotic behaviour implies that two initially close particles will separate exponentially and thus very quickly go independent pathways [19]. Small errors in initial conditions, differences in trajectory integration schemes and numerical errors amplify, such that the correlation between initial and final particle densities decays over time. This *decay of correlations* is expected to be present in a chaotic system such as the surface ocean, but to our knowledge the time scales of this process at the ocean surface have not been analyzed so far.

Understanding these time scales is important due to several reasons. From a practical perspective, specifying detailed initial particle positions is not necessary if particles are advected for much longer than the typical mixing time scale. This also means that far beyond such a time scale, initial information does not have much relevance for final particle densities, i.e. for particle distributions normalised to unity. Consequently, such a mixing time

also poses a natural limit for *backtracking*, i.e. when using Lagrangian particle tracking to investigate where plastic debris or other floating material came from. This is again illustrated in figure 2(b), where blue and red particles are mixed to length scales below the typical spatial resolution of ocean circulation models. It is then virtually impossible to accurately track individual particles back to their origin: loosely speaking, almost any origin (here east or west) within a specific basin is possible.

In this paper, we analyse the convergence to the subtropical accumulation regions and the property of mixing at the ocean surface with two methods: mixing entropy for a full time dependent particle transport model, and the concept of mixing time of the Markov chain given by the discretised transfer operator associated with the annual advective transport of particle densities. Both full particle simulations and transfer operator methods are common tools to model long term marine plastic debris transport, such that the relevance of our results can be directly interpreted within these two frameworks. Our methods reveal that on time scales of about 10-15 years, mixing is very relevant for basin scale transport simulations.

2. Methods

All methods in this paper are based on the advection of virtual passive particles constrained to the global ocean surface. Surface ocean velocity fields are obtained from a $1/12^\circ$ global NEMO ORCA-N006 simulation [20] that is forced by the Drakkar forcing consisting of wind, heat and fresh water fluxes derived from reanalysis and observed data [21]. The hydrodynamic data is provided on the ORCA grid [22]. Our dataset starts on January 5, 2000, and has a temporal resolution of 5 days. We use the Parcels framework version 1.1.0 [23] (http://oceanparcels.org) for the particle advection with the C-grid interpolation scheme described in [24]. Trajectories are integrated with the 4th-order Runge-Kutta method, with a time step of 10 minutes. Our simulations capture the transport of passive particles, i.e. we do not include any additional mechanisms of beaching, sinking or other removal from the sea surface. The code for advecting particles and for data analysis can be found on https://github.com/OceanParcels/surface_mixing. We note again that we use the term *particle density* to refer to a particle distribution *normalised to unity*.

2.1. Entropy of mixing

The entropy of mixing is the Shannon entropy [25] related to probabilities derived from spatial distributions of particles that belong to different species. It describes how well-mixed particles of different species are, i.e. how fast information on particle species is lost when transported by a given flow (see [26] and references therein).

In order to study the mixing process within each basin (see the definition of the basins in section 2.3), we start from an initially uniform distribution of particles on a global $0.2^\circ \times 0.2^\circ$ grid (approximately 1 million particles) on the beginning of our dataset (January 5, 2000), and advect them for 10 years. Each particle receives a fixed label i corresponding to its initial position within the bins of a $5^\circ \times 5^\circ$ lattice. This choice is to ensure that there are enough particles for each label to compute spatial densities based on particle statistics. It is coarser than the choice of binning for the Markov chain models, for which we are not limited by the finite number of particles (see section 2.2). Let $\rho_{i,k}(t)$ denote the discretised density of particles with label i evaluated in spatial grid cell k (taken to be $5^\circ \times 5^\circ$ as well), computed based on the particle distribution at time t. The (local) entropy of mixing at time t and bin k (called S_k(species) in [26]) is then defined as:

$$S_k(t) = -\sum_i p_{i|k}(t) \ln p_{i|k}(t), \tag{1}$$

where

$$p_{i|k}(t) = \frac{\rho_{i,k}(t)}{\sum_i \rho_{i,k}(t)}$$

is the conditional probability to find a particle of label i in a fixed bin k after advection for time t. The entropy is a measure of how strongly particles of different types are mixed within a cell k, larger values of S_k corresponding to stronger mixing. With our definition of particle labels, the entropy of mixing is a measure of the loss of the information regarding the origin of a particle. Note that we only use the densities $\rho_{i,k}$ to compute the entropy, which is independent of the actual number of particles placed in a respective bin i, as long as it is unequal of zero. Consequently, our results also apply to globally non-uniform particle distributions that initially have a non-vanishing number of particles *in each bin*.

As we are interested in the mixing property in each basin separately, we compute S_k for each individual basin by first dividing the ocean into five ocean basins (see section 2.3). This is justified by the fact that the different subtropical gyres are only weakly connected [27] on the time scales of interest for plastic transport modelling (few decades). The maximum entropy is reached for a distribution where all $p_{i|k}$ are the same and therefore equal

to $\frac{1}{M}$, where M is the number of labels in a respective basin. This yields a maximum value of $S_k^{\max} = \ln M$ for all k. Note that entirely particle depleted regions have $S_k = 0$ by definition.

2.2. Markov chain mixing

The second method is based on approximating ocean surface transport by a finite Markov chain given by a *transition matrix*. Transition matrices have been used to model passive particle advection at the ocean surface based on surface drifters [8, 9] and based on ocean circulation model output [27]. Our approach to compute the transition matrix is similar to the one of [27].

We compute a global *annual* transition matrix by advecting an initially uniform particle distribution, with particle spacing of 0.1° in longitude and latitude, for a certain time interval Δt. We then divide the ocean into N square-bins of some size $\Delta x \times \Delta x$ in longitude and latitude, and calculate the share $P_{ij}^{t\to t+\Delta t}$ of particles travelling from a bin $i = 1, ..., N$ at time t to any other bin $j = 1, ..., N$ after a time interval Δt. This share is then interpreted as the probability for a particle starting at bin i to travel to bin j in time Δt. Similar to [27], we use $\Delta t = 60$ days and $\Delta x = 2°$ for most parts of this paper, and form the product of six matrices to model the advection for 360 days: $T = P^{t_0\to t_1} \cdot P^{t_1\to t_2} \cdot \ ... \cdot P^{t_5\to t_6}$, where $t_0 =$ January 1, 2001, $t_1 = t_0 + 60$ days, $t_2 = t_1 + 60$ days, etc. For computational convenience, we model annual transport as the transport for 360 days. Note that the choice of $t_0 =$ January 1, 2001 is different from the starting time for the entropy method because we want the Markov matrix to correspond to one specific year and our dataset for the ocean current starts only on January 5, 2000. We also vary the parameters Δx, Δt and t_0 to analyse the robustness of our results.

The matrix T models the advection of a discretised particle density for one year as a stochastic Markov chain. If $\rho(t)$ is an N-dimensional row-vector representing such a density at time t (the beginning of the year), the density one year later can be computed based on the transition matrix as

$$\rho(t + 1) = \rho(t)T. \tag{2}$$

Note that transport modelling with transition matrices is expected to be more diffusive than with individual particles [28]. In addition, modelling the advection of tracers with annual transition matrices assumes the ocean current to be time-periodic. Despite these drawbacks, transition matrices take into account some of the common problems of plastic transport modelling at the ocean surface: initial conditions and the ocean currents are not known to infinite precision. In addition, tools from finite Markov chain theory are readily available to study the mixing behaviour.

From Markov chain theory, it is known (e.g. [29]) that the transition matrix has at least one *stationary density* π satisfying

$$\pi = \pi T \qquad with \quad \pi_i \geqslant 0,\ i = 1, ... N, \sum_{i=1}^{N} \pi_i = 1. \tag{3}$$

The stationary density of the Markov chain is sometimes also called *invariant measure*. If the Markov chain is irreducible and aperiodic, there is only one such stationary density and an arbitrary initial density will be attracted to this unique stationary density in the course of time [29].

For the ocean, however, each individual subtropical basin has an (approximately) invariant measure, the 'garbage patches', such that the Markov chain is not irreducible. As we are interested here in the mixing process within each individual basin, we project the transition matrix onto each basin separately (section 2.3) and normalise the rows to obtain five Markov chains, one for each subtropical basin. Each of these five Markov chains has one unique stationary density corresponding to the 'garbage patch' of the respective basin. It is important to note that the projection is an approximation, as some of the garbage patches are only approximately stationary [8, 30] in finite time (a few decades), see section 2.3.

Let Ω denote the ocean surface in a basin. The *total variation distance (TVD)* between a density ρ and π, is defined by (see e.g. [29]):

$$d(\rho, \pi) = \max_{A\subseteq\Omega} |\ \rho(A) - \pi(A)| = \frac{1}{2}\sum_i |\ \rho_i - \pi_i|. \tag{4}$$

Here, $\rho(A)$ denotes the probability to find a particle in the set $A \in \Omega$ given the probability density ρ of particles over the ocean surface Ω. As both ρ and π are densities, i.e. $\sum_i \rho_i = \sum_i \pi_i = 1$, it is easy to see that $0 \leqslant d(\rho, \pi) \leqslant 1$, where $d(\rho, \pi) = 1$ if the two densities ρ and π have disjoint support, i.e. when $\rho_i \pi_i = 0$ for every i. Also, $d(\rho, \pi) = 0$ if the densities are equal to each other. For an irreducible aperiodic Markov chain, i.e. a Markov chain with a unique invariant measure π, the distance $d(\rho(t), \pi)$ of an arbitrary initial density $\rho(t = 0)$ to the stationary density π decreases over time and converges to zero. Let δ^k denote the density with $\delta_i^k = 1$ if $i = k$ and 0 otherwise. For each k, we define the mixing time t_k as the smallest integer n (in years) that satisfies

$$d(\delta^k T^n, \pi) < \epsilon. \tag{5}$$

As is common in Markov chain theory [29], we take $\epsilon = 1/4$, but also test $\epsilon = 1/10$ to see how the mixing time changes.

Finally, it is easy to see that the maximum mixing time for all the δ^k in a basin is also the maximum for all other possible densities, as a discretised density in a fixed basin can be written as $\rho = \sum_k a_k \delta^k$, with $\sum_k a_k = 1$. Using this definition of ρ and $\sum_k a_k = 1$, it follows from the triangle inequality that

$$\begin{aligned} d(\rho T^n, \pi) &= d(\sum_k a_k \delta^k T^n, \pi) \\ &\leqslant \frac{1}{2}\sum_i \sum_k a_k |\ (\delta^k T^n)_i - \pi_i| \\ &\leqslant \sum_k a_k \max_j d(\delta^j T^n, \pi) \\ &= \max_j d(\delta^j T^n, \pi). \end{aligned} \tag{6}$$

Thus, $d(\rho T^n, \pi) \leqslant \max_k d(\delta^k T^n, \pi)$ for any ρ in a fixed basin, which means that the mixing time of an arbitrary initial density in a basin is lower or equal to the maximum mixing time of the individual δ^k. Note that in Markov chain theory, the term 'mixing time' usually refers to this maximum mixing time [29]. The stationary density π can be computed numerically from the eigenvector corresponding to the eigenvalue $\lambda = 1$ of T, cf equation (3).

We also test how well the individual stationary densities describe the final acccumlation pattern of a realistic plastic input scenario. For this, we advect the plastic inputs with the *global* transition matrix and compute basin wide densities (according to the basins defined in section 2.3) after each year. In this case, different from restricting the dynamics to the basin wide matrices, the number of particles in a basin can change over time. This is because particles that are initially outside of any basin can end up in one of the basins, and also due to connections between the different basins in the global transport matrix. We can then compute the TVD of a realistic initial plastic density in each basin advected by the Markov matrix according to equation (4).

We finally also compute a mixing entropy for the transition matrix by setting $\rho_{i,k}(t) = (T^t)_{ik}$, where t is now an integer corresponding to the number of years, which circumvents the problem of particle-depleted regions with mixing entropy $S_k = 0$ by definition (see section 2.1).

2.3. Division of the ocean surface into basins

As we wish to study the attraction to each of the individual garbage patches, we need to split up the ocean into disjoint regions and restrict the dynamics to these regions. Ideally, we would have to find the basins of attraction for each of the garbage patches. Mathematically, the basin of attraction is the region from which any particle is attracted to the attractor, i.e. each garbage patch has its own region of attraction (e.g. the North Atlantic patch has its region of attraction mostly in the North Atlantic, etc.). In our case however, the basins of attraction will only be approximations, as the 'garbage patches' themselves are only approximately stationary [8, 30]. We call our basins of attraction simply *basins* and identify them by making use of the particle dynamics instead of drawing arbitrary geographic boundaries. We find the basins through the following heuristic procedure.

For the entropy method, we divide the ocean into bins of size $2^\circ \times 2^\circ$ and compute a transition matrix P_{ij} containing the share of particles traveling from bin i to bin j in the 10-year period considered. Based on this matrix, we define the ocean basins as disjoint sets B_l defined by a set of lattice points I_l, $l = 1,...,5$ (for the five basins) such that $B_{l,i} = 1$ if $i \in I_l$ and $B_{l,i} = 0$ otherwise. These sets are chosen such that they satisfy $\sum_{j\in I_l} P_{ij} \geqslant 0.5$ for $i \in I_l$ and $\sum_{j\in I_l} P_{ij} < 0.5$ for $i \notin I_l$. In words, this means that starting within a certain basin, the probability for a particle to be in the same basin after 10 years is at least 50%. We find the sets B_l by initialising them in each basin around the garbage patches (see figure S1 available online at stacks.iop.org/ERC/1/115001/mmedia). We then compute the probability $p_{l,i}$ for each grid cell i to end up in B_l: $p_{l,i} = \sum_j P_{ij} B_{l,j}$ and add the index i to I_l if $p_{l,i} \geqslant 0.5$, and remove it if $p_{l,i} < 0.5$. We iterate this procedure until no new grid boxes are added to or removed from B_l. After defining these regions, we restrict ourselves to those particles that still are in their respective basin of origin *after each year of simulation*.

For Markov chain mixing, we compute the 10th power of the annual transition matrix, i.e. $P_{ij} = (T^{10})_{ij}$, and apply the same algorithm on P as for the entropy of mixing to determine the different regions. We choose 10 years because this is a typical time of interest for plastic transport simulations, and because for this time the North Atlantic and Arctic regions are not fully connected yet for $\Delta x = 2^\circ$ and $\Delta t = 60$ days (see figure S2 for the basins based on different powers of T). The two algorithms converge for all basins after less than 20 iterations. Figure 3 shows the final definitions of the five regions for the two methods. The two figures are very similar, apart from the Arctic which is more strongly connected to the North Atlantic for the Markov chain

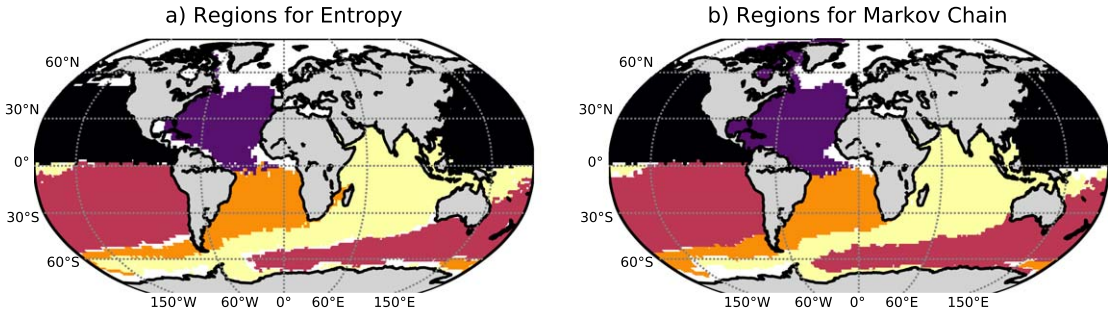

Figure 3. Definition of the separate regions for (a) entropy of mixing method and (b) Markov chain method with $(\Delta x, \Delta t) = (2°, 60 \text{ days})$.

Table 1. Parameters used in the sensitivity analysis.

Method	Case
Mixing entropy bin width	$4° \times 4°$, **$5° \times 5°$**, $6° \times 6°$
Markov chain 2001[a] $(\Delta x, \Delta t)$	$(1°, 45 \text{ days}), \epsilon = 1/4$
	$(1°, 60 \text{ days}), \epsilon = 1/4$
	$(2°, 60 \text{ days}), \epsilon = 1/4$
	$(2°, 60 \text{ days}), \epsilon = 1/10$
	$(3°, 60 \text{ days}), \epsilon = 1/4$
	$(3°, 90 \text{ days}), \epsilon = 1/4$
	$(4°, 90 \text{ days}), \epsilon = 1/4$
	$(4°, 120 \text{ days}), \epsilon = 1/4$
Markov chain 2005[b] $(\Delta x, \Delta t)$	$(2°, 60 \text{ days}), \epsilon = 1/4$

Note: All figures for the bold scenarios are in the paper.
Figures for the other scenarios are in the appendix.
[a] i.e. $t_0 =$ Jan 1, 2001.
[b] i.e. $t_0 =$ Jan 1, 2005.

method than for the entropy method. Note that the white areas in the figure, such as the Mediterranean and the Arctic, do not belong to any region.

For reference, figure S3 shows the final concentration of particles that leave their basin of origin for the full 10-year Lagrangian simulation. Figure S4 shows the share of effectively deleted particles after projecting the transition matrix for each grid cell. To assess the sensitivity of our results to the chosen parameters, we compute the entropy and transition matrix also for other choices of parameter values, shown in table 1. The definition of the basins corresponding to other parameter values for the transition matrix are shown in figure S5.

3. Results

3.1. Entropy of mixing

As mentioned, we restrict our considerations to particles that are in their respective basin of origin (shown in figure 3(a)) after each of the 10 years of simulation. For the Pacific and Atlantic basins, more than 80% of the particles remain in their respective basins during that time. Only 65% stay in the Indian Ocean, reflecting the fact that the Indian Ocean itself is relatively leaky in the long term (see also [30] and figure S2). This is also a consequence of the definition of the Indian Ocean region, which extends substantially into the Southern Ocean. We compute the spatial entropy S_k given by equation (1) and divide it by the maximum entropy of each basin, $S_k^{\max} = \ln M$. The result is shown in figure 4 for different times during the simulation. Note that the figure shows the independent entropies for each basin (according to the basin definition in figure 3(a)) in one joint global figure. As can be seen, the entropy increases during the course of the simulation to values close to 1 in a longitudinal band containing the subtropical accumulation zones. The spatial entropy is equal to its maximum in the largest parts of all basins in figure 4(c), indicating a mixing time in the order of six years. It should be noted that the entropy is close to its maximum value not only in the regions of highest accumulation, i.e. the points of highest concentration in figure 1, but also in more extensive regions spanning from west to east in each basin (as can also be seen in figure 2

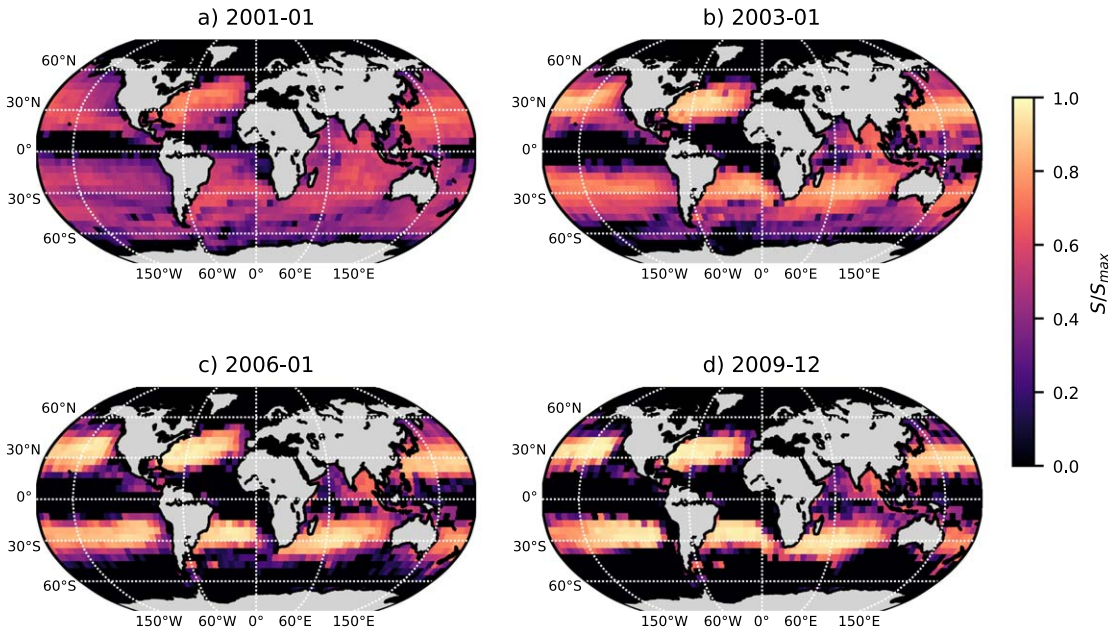

Figure 4. The spatial entropy S_k defined with a bin width 5°, scaled by the maximum entropy for each basin separately according to the definitions in figure 3(a).

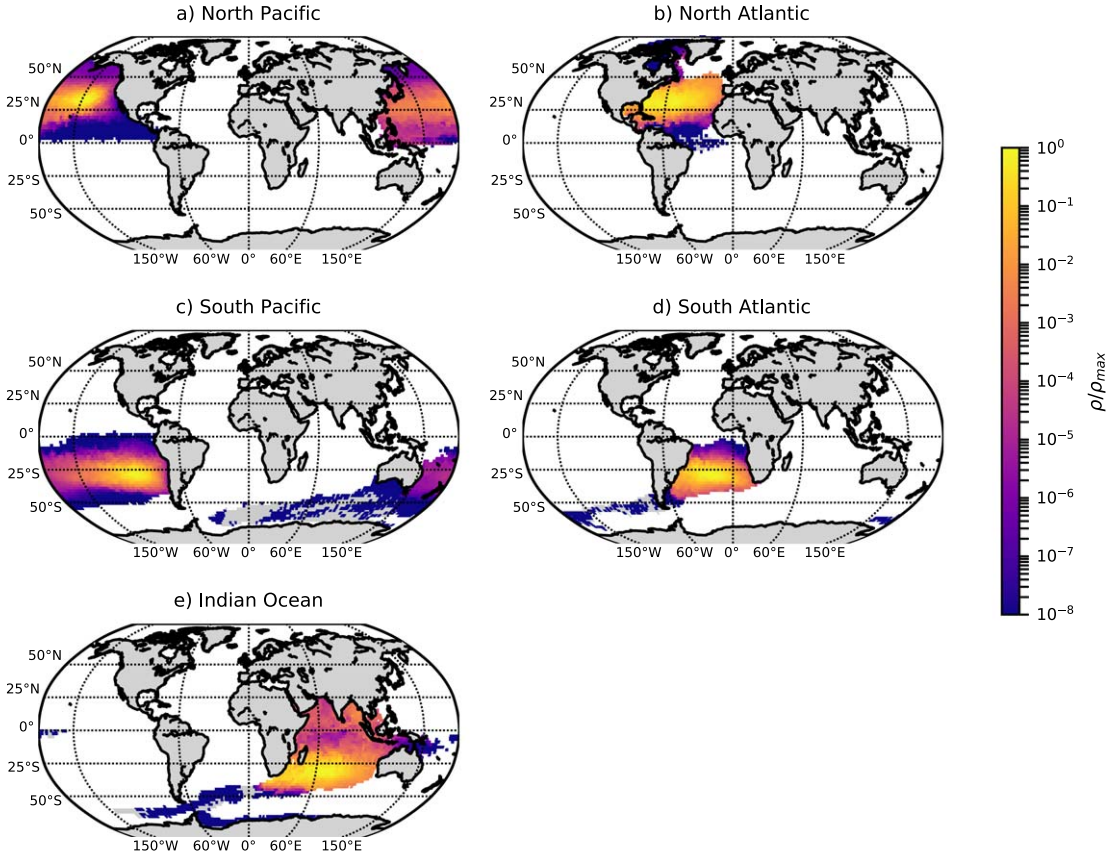

Figure 5. The stationary densities in each basin, corresponding to the eigenvector with eigenvalue 1 of T, with $(\Delta x, \Delta t) = (2°, 60 \text{ days})$. The colour shows the particle density per $2° \times 2°$ bin, normalised to the maximum density in each respective basin. Note that some bins have a stationary density of zero (e.g. close to the Southern Ocean in panels d and e) and are coloured in grey.

in the introduction for the North Pacific). Note again that a zero entropy does not mean that there is no mixing taking place at the specific location, but that there are simply no particles at these positions after some time. A change of the bin width from 5° to 4° and 6° leads to similar conclusions (see figures S6 and S7).

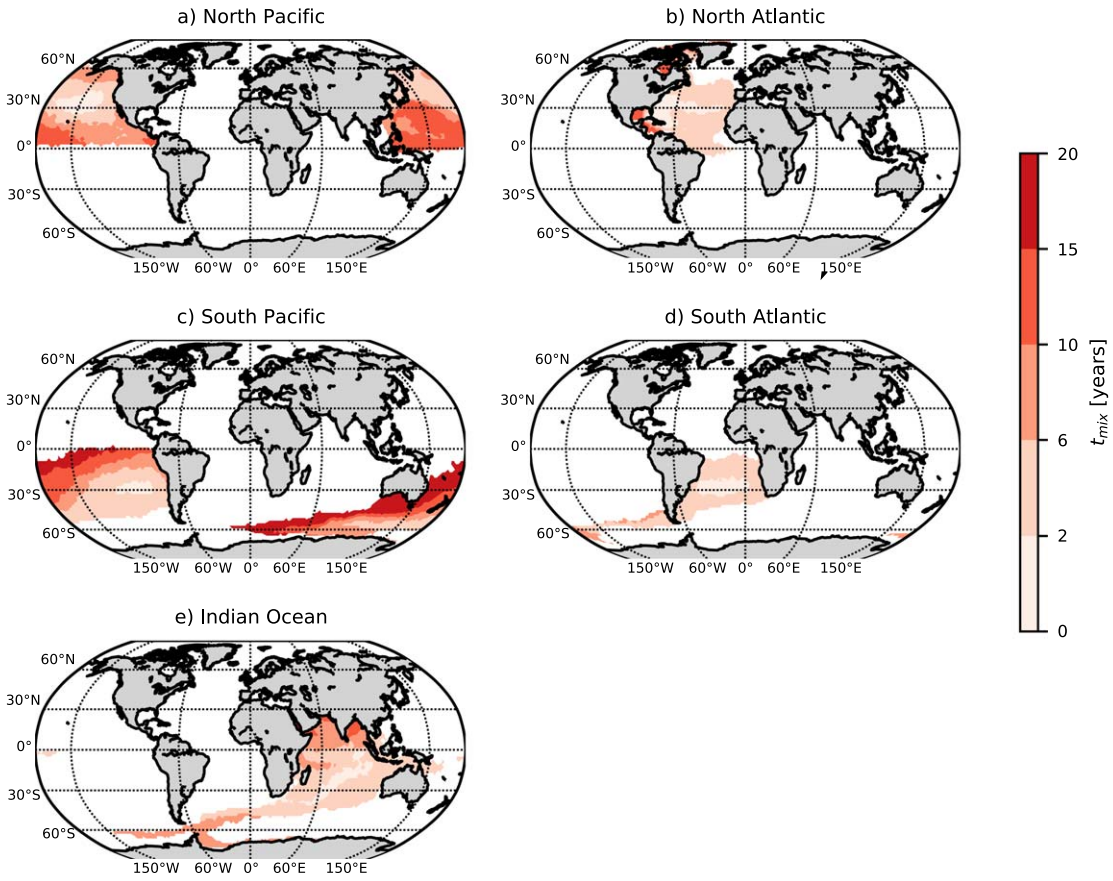

Figure 6. The Markov mixing time t_k for each basin, with $(\Delta x, \Delta t) = (2^\circ, 60 \text{ days})$.

3.2. Markov chain mixing

Figure 5 shows the stationary densities in the different basins, given by the eigenvector of T with eigenvalue 1. The regions of largest density correspond to the high accumulation regions shown in figure 1. Through our choice of basins (section 2.3), there is one unique stationary density in each of the five regions, and the individual transition matrices do not have the problem of nonphysical stationary densities close to the coasts, as was the case in [27]. The density in the North Pacific shown in figure 5 roughly corresponds to the high concentration of plastic measurements in the North Pacific, as shown in figure 1 of [12]. The same quantity in the North Atlantic seems to be slightly shifted to the west. Comparison to the other basins are difficult due to the scarcity of the data. It should be noted, however, that the densities in figure 5 are very similar to the simulation results of the 'Maximenko model' in [12], if the latter is considered in each basin separately (see their figure 3(a)). This is expected, as the stationary density corresponds to the long term evolution of an arbitrary initial density, including the uniform distribution of the 'Maximenko model' in [12], without permanent particle release. We note that the second largest eigenvalue modulus is well separated from 1 for all basins and maximal for the North and South Atlantic with $|\lambda_2| = 0.89$. Varying Δt and Δx does not result in a strong obvious change of the stationary densities (see figures S8–S14).

Figure 6 shows the mixing time t_k defined through equation (5) for each bin of the ocean surface. The mixing time for the other transition matrices are shown in figures S15–22 in the appendix. For $\epsilon = 1/4$, around 70% of the covered ocean surface has mixing times of 10 years or less, and this does not change for other parameter choices of $(\Delta x, \Delta t)$ (see figure S23). Note that this excludes the part of the ocean that is not part of any basin, e.g. the Artic in figure 3. The time scale of 10 years is comparable to or shorter than the typical time scale of simulation in many plastic transport models, which is typically in the order of a few decades [8–13]. Some regions in figure 6, in particular parts of the North Pacific and South Pacific, have higher mixing times of more than 10 years. Remarkably, it is also visible in figure 6 that mixing times do not become larger towards land. This means that within the probabilistic description of ocean transport based on a transition matrix, particles with initial positions close to land are equally mixed over the respective attractor as particles starting in the open ocean. The low value of mixing time in the largest parts of the global ocean indicates that the convergence

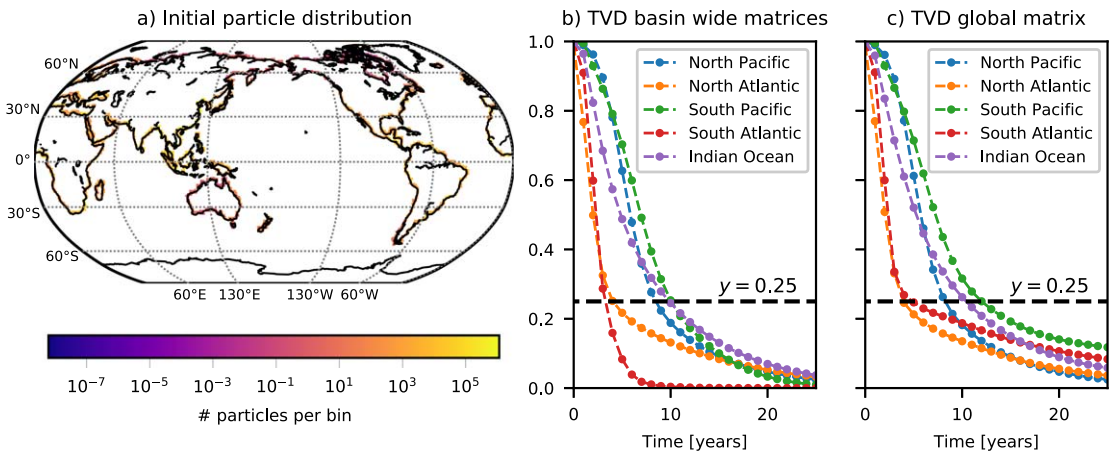

Figure 7. (a) Plastic input scenario of the 'van Sebille model' in [12]; (b) TVDs for the different basins, with dynamics restricted to the individual basins; (c) TVDs of the basin wide densities from the full dynamics, cf section 2.2.

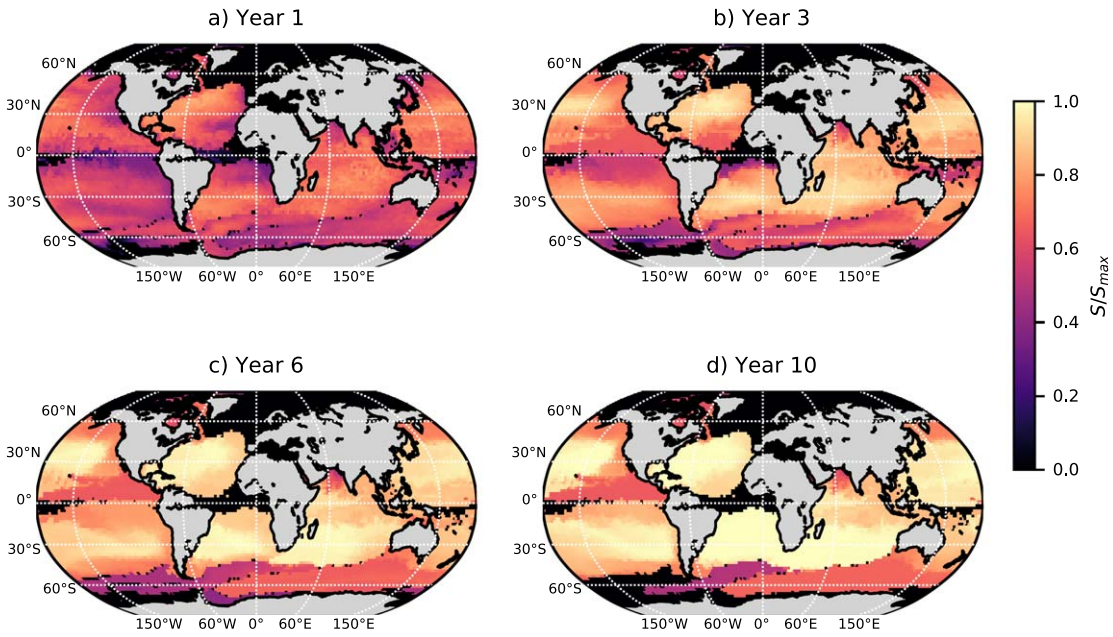

Figure 8. Entropy S_k computed from the transport given by the Markov matrix T, with $(\Delta x, \Delta t) = (2°, 60 \text{ days})$.

towards the garbage patches happens on relatively fast time scales. Setting $\epsilon = 1/10$ in equation (5) changes the mixing times of course, but still more than 70 % of the covered ocean surface has a mixing time of 15 years or less (see figures S22–23).

We wish to emphasise that the maximum Markov mixing time is also the maximum mixing time for any arbitrary initial particle density in the basin, when the dynamics is restricted to that particular basin, as was demonstrated in equation (6).

We now look at the advection of a realistic plastic input scenario, used in the 'van Sebille model' in [12], shown in figure 7(a). We first advect this input scenario (given on a 1° grid) with the *basin wide* projected transition matrices of $(\Delta x, \Delta t) = (1°, 60 \text{ days})$ and compute the TVD for each year and each basin to the corresponding stationary densities. By doing so, we exclude all the particles that are not initially placed in one of the five regions (see figure S3b). The resulting TVDs are shown in figure 7(b). We see that the TVD decreases over time and tends towards zero for all basins. Figure 7(c) shows the TVDs of the full initial particle distribution advected by the global transition matrix to the densities in each basin (cf section 2.2). The mixing times in figure 7(c) are slightly larger than in figure 7(b). This is expected, as we also include initial positions of particles that are not part of a basin. In addition, the individual basin wide stationary densities can together only

approximate a global stationary density because interconnections between the different basins exist in the global transition matrix, and because some particles. The restriction to the basins for figure 7(c) leads to a reduction of the total number of particles to about 77%. The remaining 23% are mostly in the Artic and Mediterranean after 25 years of advection, see figure S24. The mixing time according to figure 7(c) is still less than 15 years, much smaller than the maximum mixing time for the matrix with $(\Delta x, \Delta t) = (1^\circ, 60 \text{ days})$, which is 25 years (see table 1 in the supplementary material). This also shows that our restriction to separately study the mixing property of the individual basins is justified.

To test the sensitivity of our results on the choices of spatial and temporal resolution Δx and Δt, we determine the mean mixing time for $\epsilon = 1/4$, $t_0 = 2001$ for each of the Markov matrices in each basin (table 1 in the supplementary material). In all basins except for the North Atlantic, there is a trend for the mean mixing time to become smaller for larger Δx, roughly decreasing by one year or less when increasing Δx by 1° in our models. This is intuitive, as larger spatial binning introduces stronger randomization and thus diffusion in the dynamics, such that densities are expected to mix more quickly [28]. Again in all basins but the North Atlantic, the mean mixing time becomes larger with larger Δt, with a maximum of 0.6 years increase when increasing Δt by 30 days. This is again intuitive, as the construction of an annual matrix with a larger Δt requires less matrix multiplications, causing less randomization across grid cells. The North Atlantic plays a somewhat special role, showing no clear dependence of Δx or Δt. Hence, the average mixing time does not change very strongly (order of 1–2 years) when changing the parameters for the Markov matrices (see also figure S23 in the appendix).

The mixing entropy based on the transition matrix by setting $\rho_{i,k}(t) = T^t_{i,k}$ (cf section 2.2) is shown in figure 8. We see that the mixing entropy is at its maximum in most parts of the ocean after 10 years, also containing regions which were black in figure 4 because of the lack of particles. It is interesting to note that the parts of the Southern Ocean that are included in this study keep a relatively low value for the entropy, as does the southeastern part of the North Pacific. This indicates that these regions have mainly outflow into the rest of the respective basin, but only little inflow.

4. Conclusion

The chaotic transport of passive particles by the surface ocean is highly sensitive to the choice of initial particle positions and errors in particle advection models. Tracers transported by the ocean currents are therefore mixed in space, and their trajectories gradually loose the correlation to their initial particle positions. On the time scale of several decades, particle clouds are attracted to the subtropical accumulation zone in each ocean basin and are dispersed over the attraction region, almost independent of their initial position.

We used the methods of mixing entropy and Markov chain mixing computed from an annual transition matrix representing the surface flow to analyse the typical mixing time scales of tracers at the ocean surface. All our results are limited to basin scale long term modelling of a few years to decades, and neglect the possibility of a particle to sink or beach, as is similar to previous studies [8, 9, 12, 13]. We apply our methods to individual subtropical basins in order to capture the main dynamics in this time range. Based on a fully time dependent transport model, the entropy method showed that particles from different origins are almost completely mixed after approximately six years in the largest regions of the subtropical basins. The Markov chain method revealed that, while some regions in particular in the northern South Pacific have mixing times of more than 20 years, the mixing times are in the order of or below 10 years for 70% of the covered surface ocean area.

The effect of mixing and history loss of passive tracers is relevant and needs to be considered for global Lagrangian particle simulations at the ocean surface, in particular if initial particle positions are correlated with final distributions. This applies in particular to plastic transport modelling, where simulation times are typically in the order of a few decades, i.e. precisely when mixing is relevant. From an environmental perspective, our findings imply that plastic is transported over the entire accumulation zone within a time scale of about 10-15 years, regardless of the sources. Consequently, mitigating marine plastic pollution needs common efforts of all neighbouring countries. Yet, our 'plastic particles' are passive particles at the ocean surface, which is an incomplete model of real plastic particles. To model realistic plastic particles and analyse their transport and fate is still one of the major challenges in the plastic community, and the global mixing properties of real plastic might be different from the findings presented here.

It should be noted that our results on mixing apply solely to basin wide long term transport processes, where particle distributions converge to the respective attractors, i.e. we neglect transient behaviour. On more local scales and shorter time scales, initial particle locations will matter, and realistic input scenarios can be very relevant for transport pathways and final distributions.

The mixing property analysed in this study is mainly a consequence of incomplete knowledge of initial particle positions and the ocean circulation. We parameterised these uncertainties in an abstract manner by the choices of labels for the entropy method, and the spatial binning and time step for the Markov chain

approximation. These parameters are clearly choices, but we find that the spatial distribution of Markov chain mixing times is only weakly affected by changes in these parameters. Further research is needed to actually quantify the amount of uncertainty that is present in the results of Lagrangian particle modelling, which is a combination of uncertainties from initial conditions and the ocean current data. Yet, regardless of the level of uncertainty present in particle advection models, the ocean surface transport will possess the mixing property due to the chaotic nature of the ocean flow. The presence of mixing needs to be carefully taken into account in the interpretation of results from Lagrangian particle trajectories.

The mixing time that arises from these uncertainties sets a time scale after which initial conditions only have limited influence on final particle densities. Consequently, our results also have important implications for backtracking of individual plastic particles: as any initial particle distribution in a basin is attracted to the respective stationary density, the information of the precise initial distribution is lost over time. On the basin scale it is therefore virtually impossible to infer an initial distribution from a final distribution if the latter is close to the stationary density.

Acknowledgments

David Wichmann, Philippe Delandmeter and Erik van Sebille are supported through funding from the European Research Council (ERC) under the European Union Horizon 2020 research and innovation programme (grant agreement No 715386). This work was carried out on the Dutch national e-infrastructure with the support of SURF Cooperative (project no. 16371). We thank Andrew Coward for providing the ORCA-N006 simulation data.

ORCID iDs

David Wichmann https://orcid.org/0000-0001-5530-8377
Philippe Delandmeter https://orcid.org/0000-0003-0100-5834
Erik van Sebille https://orcid.org/0000-0003-2041-0704

References

[1] Barnes D K A, Galgani F, Thompson R C and Barlaz M 2009 Accumulation and fragmentation of plastic debris in global environments *Philosophical Transactions of the Royal Society B: Biological Sciences* **364** 1985–98
[2] Cozar A *et al* 2014 Plastic debris in the open ocean *Proc. Natl Acad. Sci.* **111** 10239–44
[3] Derraik J G B 2002 The pollution of the marine environment by plastic debris: a review *Marine Pollution Bulletin* **44** 842–852
[4] Cole M, Lindeque P, Halsband C and Galloway T S 2011 Microplastics as contaminants in the marine environment: a review *Marine Pollution Bulletin* **62** 2588–2597
[5] Jambeck J R, Geyer R, Wilcox C, Siegler T R, Perryman M, Andrady A, Narayan R and Law K L 2015 Plastic waste inputs from land into the ocean *Science* **347** 768–71
[6] Lebreton L C M, Van Der Zwet J, Damsteeg J W, Slat B, Andrady A and Reisser J 2017 River plastic emissions to the worldas oceans *Nat. Commun.* **8** 15611
[7] Hardesty B D, Harari J, Isobe A, Lebreton L, Maximenko N, Potemra J, van Sebille E, Vethaak A D and Wilcox C 2017 Using numerical model simulations to improve the understanding of micro-plastic distribution and pathways in the marine environment *Frontiers in Marine Science* **4** 30
[8] van Sebille E, England M H and Froyland G 2012 Origin, dynamics and evolution of ocean garbage patches from observed surface drifters *Environ. Res. Lett.* **7** 44040
[9] Maximenko N, Hafner J and Niiler P 2012 Pathways of marine debris derived from trajectories of Lagrangian drifters *Mar. Pollut. Bull.* **65** 51–62
[10] Lebreton L C M, Greer S D and Borrero J C 2012 Numerical modelling of floating debris in the world's oceans *Mar. Pollut. Bull.* **64** 653–61
[11] Eriksen M, Lebreton L C M, Carson H S, Thiel M, Moore C J, Borerro J C, Galgani F, Ryan P G and Reisser J 2014 Plastic pollution in the world's oceans: more than 5 trillion plastic pieces weighing over 250,000 tons afloat at sea *PLoS One* **9** e111913
[12] van Sebille E, Wilcox C, Lebreton L, Maximenko N, Hardesty B D, Van Franeker J A, Eriksen M, Siegel D, Galgani F and Law K L 2015 A global inventory of small floating plastic debris *Environ. Res. Lett.* **10** 124006
[13] Lebreton L *et al* 2018 Evidence that the Great Pacific Garbage Patch is rapidly accumulating plastic *Sci. Rep.* **8** 4666
[14] Kubota M 1994 A mechanism for the accumulation of floating marine debris north of hawaii *J. Phys. Oceanogr.* **24** 1059–64
[15] van Sebille E 2015 The oceans' accumulating plastic garbage *Phys. Today* **68** 60–1
[16] Ye S and Andrady A L 1991 Fouling of floating plastic debris under Biscayne Bay exposure conditions *Mar. Pollut. Bull.* **22** 608–13
[17] Kaiser D, Kowalski N and Waniek J J 2017 Effects of biofouling on the sinking behavior of microplastics *Environ. Res. Lett.* **12** 124003
[18] Fazey F M C and Ryan P G 2016 Biofouling on buoyant marine plastics: an experimental study into the effect of size on surface longevity *Environ. Pollut.* **210** 354–60
[19] LaCasce J H 2008 Statistics from Lagrangian observations *Prog. Oceanogr.* **77** 1–29
[20] Madec G and and the NEMO team 2008 NEMO ocean engine *Note du Pôle de modélisation, Institut Pierre-Simon Laplace (IPSL), France* No. 27
[21] Dussin R, Barnier B, Brodeau L and Molines J M 2016 The making of Drakkar forcing set DFS5 *DRAKKAR/MyOcean*
[22] Madec G and Imbard M 1996 A global ocean mesh to overcome the North Pole singularity *Clim. Dyn.* **12** 381–8

[23] Lange M and van Sebille E 2017 Parcels v0.9: prototyping a Lagrangian ocean analysis framework for the petascale age *Geoscientific Model Development* **10** 4175–86
[24] Delandmeter P and van Sebille E 2019 The Parcels v2.0 Lagrangian framework: new field interpolation schemes *Geoscientific Model Development* **12** 3571–3584
[25] Shannon C E 1948 A mathematical theory of communication *Bell Syst. Tech. J.* **27** 379–423
[26] Camesasca M, Kaufman M and Manas-Zloczower I 2006 Quantifying fluid mixing with the shannon entropy *Macromol. Theory Simul.* **15** 595–607
[27] Froyland G, Stuart R M and van Sebille E 2014 How well-connected is the surface of the global ocean? *Chaos* **24** 033126
[28] McAdam R and van Sebille E 2018 Surface connectivity and interocean exchanges from drifter-based transition matrices *Journal of Geophysical Research: Oceans* **123** 514–32
[29] Levin D A, Peres Y and Wilmer E L 2009 *Markov chains and mixing times* (Providence: American Mathematical Society)
[30] van der Mheen M, Pattiaratchi C and van Sebille E 2019 Role of indian ocean dynamics on accumulation of buoyant debris *Journal of Geophysical Research: Oceans* **124** 2571–90